IEEE Open Journal of Intelligent Transportation Systems

This article has been accepted for publication in IEEE Open Journal of Intelligent Transportation Systems. This is the author's version which has not been fully edited and content may change prior to final publication. Citation information: DOI 10.1109/OJITS.2026.3713602

Received XX Month, XXXX; revised XX Month, XXXX; accepted XX Month, XXXX; Date of publication XX Month, XXXX; date of current version XX Month, XXXX.

Digital Object Identifier 10.1109/OJITS.2022.1234567

Driver Visual-Cognitive Distraction Monitoring: The VICODEV Index

LORENZO UCCELLO[1], LUCA SUBITONI[2], MASSIMILIANO GOBBI[1], MARIA G. SIGNORINI[2], GIANPIERO MASTINU[1]

[1]Department of Mechanical Engineering, Politecnico di Milano, Milan, 20156 Italy
[2]Department of Electronic, Information and Bioengineering (DEIB), Politecnico di Milano, Milan, 20154 Italy

CORRESPONDING AUTHOR: Lorenzo Uccello (e-mail: lorenzo.uccello@polimi.it).

This work was funded partially by EU – NextGenerationEU, M4C2 I1.1, Progetto PRIN 2022 “HL4IT”, Prot.2022L3M25K – CUP D53D23003750006, and partially by EU – NextGenerationEU, M4C2 I1.1, Project PRIN 2022 PNRR ”STAVE”, Prot. P2022KSN9Z, CUP D53D23016080001.

ABSTRACT This work introduces “VIsual-COgnitive Distraction through Eye-tracking and Vehicular measurements” (VICODEV), an interpretable, statistically driven index combining five vehicular and behavioural measurements to estimate induced visual-cognitive distraction. The index was developed through an experimental campaign at the dynamic driving simulator of Politecnico di Milano using an Instrumented Steering Wheel, eye-tracking glasses, an electroencephalograph, and an electrocardiograph. Thirty-five novice drivers were recruited for the tests. Alongside the primary driving task, drivers performed five repetitions of a secondary “Clock Task”, inducing visual-cognitive distraction. During each secondary task, participants solved mathematical operations displayed on a tablet inside the cockpit. Twenty-one measurements were collected to describe induced distraction, including vehicular, behavioural, and physiological types. The Wilcoxon Signed Rank Test revealed twelve measurements with statistically significant trends between normal and induced distracted driving. Five measurements were then selected considering real-time in-vehicle applicability, namely Standard Deviation of Lateral Position of the vehicle’s center of gravity to the lane centerline, standard deviation of steering wheel grip force, Eyes Off-Road Time, rate of high-velocity eye movements, and mean duration of low-velocity eye movements. VICODEV combines these five measurements via canonical discriminant analysis, assessing induced visual-cognitive distraction every 40 ms. Leave-one-repetition-out cross-validation achieved an average recall of 99.47% and accuracy of 95.20%, confirming the index consistency across secondary task repetitions. Leave-one-subject-out cross-validation yielded a median Area Under the Receiver Operating Characteristic Curve of 82.9%, showing the index’s ability to identify shared patterns across the tested population. This study offers a standardised reference to support DMS design, evaluation, and comparison.

INDEX TERMS driver distraction, cognitive workload, driving simulator, DMS, DCAS, ADAS, human factors, attention.

I. INTRODUCTION

DRIVER distraction is a leading contributor to road accidents worldwide, playing a significant role in traffic-related fatalities and injuries [1]. To mitigate human error, the automotive industry has increasingly adopted Advanced Driver Assistance Systems (ADAS) and progressively introduced partially Automated Driving (AD) technologies [2]. Maintaining continuous driver engagement has become a critical challenge in modern vehicle design. This is especially true given the diverse Non-Driving Related Tasks (NDRTs) with respect to automation levels [3], [4]. Consequently, Driver Monitoring Systems (DMS) have acquired a key role in Driver Control Assistance Systems (DCAS). United Nations Economic Commission for Europe (UNECE) Regulation No.171 has mandated the integration of driver engagement monitoring in DCAS [5]. The European New Car Assessment Protocol (Euro NCAP) 2030 roadmap called for the development of Direct Driver Monitoring Systems to assess driver state, paving the way toward cognitive distraction [6]. This research aims to investigate the effects

This work is licensed under a Creative Commons Attribution 4.0 License. For more information, see https://creativecommons.org/licenses/by/4.0/

of visual-cognitive distraction induction as a precursor to full cognitive distraction. To this end, the "VIsual-COgnitive Distraction through Eye-tracking and Vehicular measurements" (VICODEV) index is proposed, adopting a multidisciplinary and hypothesis-driven method.

Understanding distraction requires a clear definition of attention and its intrinsic limitations. Indeed, attention is a limited resource, allowing individuals to select and process relevant environmental stimuli [7]. In the driving context, distraction occurs when attention is diverted from the primary driving task to a secondary task. According to the National Highway Traffic Safety Administration (NHTSA), distraction can be classified into four categories [8].

- Visual distraction (e.g., looking away from the road).
- Auditory distraction (e.g., responding to non-driving-related sound stimuli).
- Biomechanical or motor distraction (e.g., manipulating objects).
- Cognitive distraction (e.g., mind wandering).

Within this context, visual-cognitive distraction can be considered a hybrid category of distraction. Specifically, secondary tasks require drivers to look away from the road not only to retrieve visual information but also to process it (e.g., for mathematical calculations or logical associations), thereby increasing cognitive workload. In this research, the well-known Clock Task is employed to induce drivers' visual-cognitive distraction [9], combining both visual diversion and mental arithmetic.

A wide range of measurements has been explored in the literature to capture distraction complexity [10]. These are generally grouped into four distinct types [11], [12].

- Vehicular measurements, which monitor vehicle motion, such as variations of speed or lateral position of the vehicle's center of gravity.
- Behavioural measurements, which focus on observable driver actions, including gaze and hand movements.
- Physiological measurements, which reflect internal conditions, such as variations in heart rate or brain activity.
- Subjective measurements, which collect self-reported data from drivers, offering insights into perceived workload and task difficulty.

This study adopts an extended testbed, consisting of a highly realistic dynamic driving simulator equipped with a proprietary Instrumented Steering Wheel (ISW), Eye-Tracking glasses, an Electrocardiograph (ECG) and an Electroencephalograph (EEG). Hence, this testbed allows the retrieval of vehicular, behavioural and physiological measurements. Furthermore, the testbed has been expanded to collect subjective measurements. To this end, the Attention Network Test (ANT) assesses participants' attentional skills, and the NASA Task Load Index (NASA-TLX) measures the perceived workload during the whole test. In this work, subjective measurements are used as informative experimental feedback on the induced visual-cognitive distraction.

Recent studies highlight the importance of hybrid measurements, which combine several types of measurements to enhance sensitivity and robustness in distraction estimation [13], [14]. Examples of hybrid measurements include the combination of behavioural and physiological measurements, such as gaze patterns and electroencephalographic (EEG) or electrocardiographic (ECG) signals [15]. The coupling of physiological and vehicular measurements is another example, which led to EEG activity being linked to metrics like brake reaction time and steering entropy [16]. Despite employing hybrid approaches, most distraction detection methods tend to simplify the problem of driver distraction. Specifically, these methods consider binary classification tasks, distinguishing only between "normal" and "distracted" driving states. While this dichotomy enables straightforward model training and evaluation, it may fail to capture the dynamic nature of human attention [17]. In response to this limitation, distraction assessment frameworks have been developed. These frameworks identify distraction categories, relate measurements to actions performed by drivers during distraction, and quantify the associated risk levels [18], [19].

Recent studies in driver distraction and attention modelling integrate both gaze estimation and scene analysis [20], [21]. Within this context, authors in [20] proposed a deep neural network to predict a probabilistic visual map of the driver's gaze. The network was trained by fusing head pose and eye appearance information from single-frame inputs. Building on this perspective, other works have emphasised the importance of modelling driver attention dynamically, both over time and across the spatial structure of the driving scene. In particular, authors in [21] proposed the use of a multi-scale temporal-spatial fusion network for driver attention prediction. This model combined extracted features through an attention-guided fusion strategy. Authors showed that effective driver attention prediction benefits from models that not only extract measurements but also flexibly weight their importance. Other recent approaches have explored deep learning architectures of increasing complexity. For example, authors in [22] proposed a weakly-supervised contrastive learning framework to detect and quantify motor distractions. While achieving accurate driver activity recognition, this approach relies on compressed latent representations and on images captured by in-cockpit cameras. This may limit the interpretability of the model and its applicability to visual-cognitive distraction.

In this research, VICODEV is an interpretable index which weights vehicular and behavioural measurements, selected for their real-world availability through sensors suitable inside the vehicle. Moreover, the VICODEV index provides a continuous output value, potentially supporting continuous monitoring of driver distraction over time. Finally, this research assumes that distraction cannot be uniformly estimated across individuals. The experimental protocol induces visual-cognitive distraction, which may be managed differently by subjects. Thus, the VICODEV index

This article has been accepted for publication in IEEE Open Journal of Intelligent Transportation Systems. This is the author's version which has not been fully edited and content may change prior to final publication. Citation information: DOI 10.1109/OJITS.2026.3713602

is designed mainly to capture consistent response patterns across the subject population.

The paper is organised as follows. Section II details the experiment procedure, testbed and participant pool. Section III describes the data acquisition process and the definition of measurements. Section IV illustrates the statistical and descriptive analyses. Section V introduces and validates the proposed VICODEV index.

II. EXPERIMENT

A. Procedure

The experimental campaign was conducted using the dynamic driving simulator at the DriSMi Laboratory of Politecnico di Milano [23], shown in Figure 1b. Participants drove within a simulated environment replicating a district of Wolfsburg, Germany, shown in Figure 1a. The scenario consisted of a two-lane urban road in each direction, extending over a total distance of 4.1km and populated with 107 vehicles, corresponding to a vehicle density of about 26 vehicles/km.

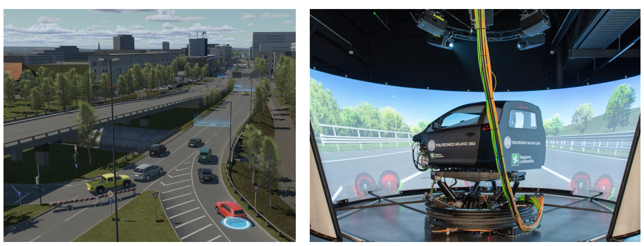

(a) (b)

FIGURE 1: (a) Simulation scenario developed in VI-Worldsim. The red car on the right is the one driven by participants. As soon as participants merge onto the main road, they must keep the leftmost lane for the entire simulation and follow the preceding vehicle. (b) DriSMi dynamic driving simulator (DiM400), Politecnico di Milano.

Each simulation session lasted approximately 9 minutes. Figure 2 shows the complete set of phases of the experiment. At the beginning of the simulation, participants drove in the leftmost lane. This starting phase (S) also served to initialise sensors and verify their correct functioning. The experiment proceeded with five Baseline (i.e., normal driving, B) phases, alternating with five induced Distraction (D) phases, each lasting 45 seconds. At the end of the simulation (E), participants were instructed to return to the rightmost lane and safely stop the vehicle.

An auditory cue notified the start of each phase of visual-cognitive distraction induction. Specifically, visual-cognitive distraction was elicited employing a *Clock Task* [9], [24]. During the Clock Task, the vehicle dashboard positioned on the right-hand side was used to display a sequence of six clocks. This configuration has been chosen to increase the Clock Task ecological validity, recreating the interiors and infotainment system of a real vehicle. The dynamic driving simulator further improves realism, when compared

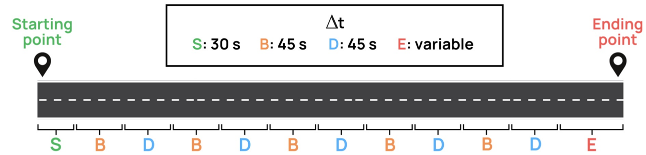

FIGURE 2: Sequence of driving phases of the experiment. Five Baseline (B) alternated with five induced distraction (D) driving phases, each lasting 45 seconds. S and E refer to the starting and ending driving phases, respectively.

to widely adopted laboratory static simulators. Figure 3a shows the drivers' point of view inside the dynamic driving simulator cockpit. Drivers were required to sum the numbers indicated by the clock hands and verbally report the result following a visual prompt. Each clock featured numbers ranging from 13 to 24. To progressively increase the cognitive and visual load, visual complexity was varied across clocks through their primary characteristics, such as colour changes, number dimension variations, and the use of Roman numerals [25]. The long-term learning effect characterising mathematical calculations has been limited by changing clocks across all repetitions. The duration of the clock display varied from 3 to 7 seconds, depending on the clocks' complexity, to further limit the learning effect and make the task more challenging. Figure 3b presents an example of a clocks' display sequence.

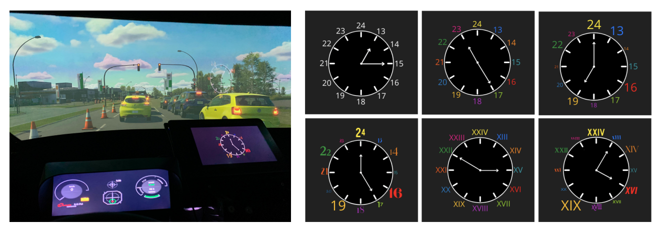

(a) (b)

FIGURE 3: (a) Driver's point of view inside the cockpit. From left to right, the vehicle dashboard and the tablet showing the clocks. (b) Example of a sequence of 6 clocks shown to the driver during visual-cognitive distraction.

Before starting the experiment, drivers were instructed to maintain their lane and avoid overtaking or turning manoeuvres, simplifying the primary driving task to a car-following scenario. This ensured that potential differences between the experimental phases could be attributed to the secondary task rather than to varying driving demands. The use of a dynamic driving simulator allowed this controlled scenario to be embedded in a realistic urban environment, while maintaining safety requirements and repeatability that would not be achievable in real-world studies. Moreover, before the simulation, participants also performed the Attention Network Test (ANT) [26], a cognitive assessment used to assess the subjects' attentional skills. After the simulation, they completed the NASA-TLX questionnaire [27], a widely used tool for evaluating perceived workload during the simulation across six dimensions, including mental demand, physical demand, and effort.

Finally, participants wearing the EEG were instructed to limit head movements during the simulation to reduce motion-related EEG artefacts, while preserving natural behaviour. No participant subjectively reported the instruction as restrictive, and no participant was excluded for non-compliance. To assess objectively whether this instruction led to atypical behaviour, the Root-Mean-Square (RMS) of the resultant head acceleration (i.e., Euclidean norm of the three components from the eye-tracker accelerometer) was analysed at two levels. A between-subjects comparison during distraction showed no significant difference between the no-EEG (median = 1.0018 m/s², IQR = 0.572 m/s²) and EEG populations (median = 1.3149 m/s², IQR = 1.108 m/s²) (Mann–Whitney U test, p = 0.0963). A within-subject Wilcoxon signed-rank test between baseline (B) and distraction (D) phases yielded no significant difference in either group (EEG: p = 0.640; no-EEG: p = 0.931). The absence of head-movement changes reflects the task design. The Clock Task is displayed on the in-cockpit tablet within the driver's forward field of view, as shown in Figure 3a. Therefore, the gaze shift required lies within the oculomotor range without needing head rotation.

B. Testbed

1) Dynamic Driving Simulator

The primary testbed component is the Dynamic Driving Simulator of the DriSMi laboratory [23]. The DiM400 developed by VI-Grade and Politecnico di Milano features a two-stage actuation system. The first stage is represented by a cable-driven platform allowing horizontal plane motion (i.e., 4×4 meters displacement, $\pm60^\circ$ yaw). The second stage comprises a hexalift providing six degrees of freedom up to 30Hz. Eight shakers supply high-frequency vibrations (i.e., up to 200Hz). The simulator offers a 270° high-definition visual system, active seat belts, an active brake pedal, and an instrumented cockpit based on a real vehicle frame. Total system latency is below 20ms, ensuring high immersion and realistic driving feedback. The driving simulator virtual Controller Area Network (CAN) is written in a Real-time Database (RtDb) which can be accessed during and after the simulation for data retrieval. Additional information regarding the dynamic driving simulator is detailed in [28].

2) Sensors

An acquisition setup was used to monitor vehicular dynamics and drivers' behaviour and physiological state. Sensors are divided into two groups.

- Integrated sensors, directly linked to the Real-Time Database (RtDb) of the simulator, including vehicular CAN signals, the Instrumented Steering Wheel (ISW), and the Electrocardiograph (ECG).
- External sensors, requiring time synchronization via a digital trigger signal, comprising the Eye-Tracking glasses and the Electroencephalograph (EEG).

The sensors and their characteristics are reported below.

- *Instrumented Steering Wheel (ISW)* — A proprietary device developed at Politecnico di Milano [29]. The ISW features two handles, equipped respectively with three mono-axial load cells and a six-axis load cell. Data was acquired at 1000Hz via CAN interface.
- *Eye Tracker* — Tobii Pro Glasses 3 wearable glasses-based system, operating at 25Hz. The system estimates the 3D gaze direction.
- *Electrocardiograph (ECG)* — A three-lead ECG sensor directly integrated into the dynamic driving simulator network, with a sampling rate of 1000Hz.
- *Electroencephalograph (EEG)* — A multi-channel EEG system developed by ANT Neuro (NA-261-waveguard™ net). It consists of (64+1) electrodes arranged in an equidistant layout which are prepared using a saline-based conductive solution. Scalp potentials are recorded at 1000Hz.

This integrated sensor configuration ensured consistent temporal alignment across the simulation, allowing robust data collection during all driving phases.

C. Participants

An a priori power analysis was conducted to determine the minimum sample size. The Standard Deviation of Lateral Position (SDLP) was selected as the primary outcome, given its widespread use as a benchmark metric in lane-keeping and distraction studies. Considering results in [30], drivers exposed to distraction in urban environments performed worse in terms of straight-line driving. Specifically, SDLP changed from $\mu \pm \sigma$ = 0.67 $\pm$ 0.35m (normal driving) to $\mu \pm \sigma$ = 0.84 $\pm$ 0.31m (distracted driving), corresponding to $\Delta SDLP$ = 0.17m. A paired-samples t-test was assumed, considering a moderate within-subject correlation ($\rho = 0.5$) between baseline (B) and induced distraction (D), a significance $\alpha = 0.05$, and a power $(1-\beta) = 0.80$, yielding a required sample size of N = 30 participants. As a result, 35 participants (i.e., 21 males and 14 females) were recruited.

The test population represents young and novice drivers with limited driving experience, thus isolating demographic effects [13]. Participants' ages ranged between 19 and 30 years (*Mean*: 22.9 years, *SD*: 2.39 years), and all held a valid driving license for at least one year. Self-reported annual driving mileage varied considerably, with the majority of participants reporting less than 5,000 km per year. 19 participants were instrumented with the EEG device. A preliminary screening was performed to verify EEG signal quality and ensure participant suitability. Subjects 11 and 15 completed four of the five induced distraction driving phases, and subject 23 completed only three due to motion sickness.

Before starting the simulation, participants signed an informed consent form, detailing the test objective, sensors used and data retrieval and storage. The study received approval by the Ethics Committee of the Politecnico di Milano no. 16/2023 issued on 5 May 2023.

III. Data processing

Table 1 lists the twenty-one measurements retrieved during the experimental campaign, categorised as vehicular, behavioural and physiological measurement types. These measurements were selected either for their frequent use in studies on visual-cognitive distraction or because they showed consistent and significant trends in similar research, as reported in Table 1. Specifically, measurements were extracted from two distinct driving phases, each defined within a 30-second analysis window. 15 seconds per driving phase have been discarded to avoid carry-over effects from previous repetitions.

1) *Non-induced distraction driving, baseline (B)*: the time interval before the start of the distraction induction provided by the secondary clock task.

2) *Driving during distraction induction (D)*: the time interval during the distraction induction via the clock task, measured from the auditory cue signalling the start of the secondary task.

A. Vehicular measurements

Vehicular measurements were pre-processed to isolate visual-cognitive distraction effects, minimising confounding influences such as traffic or environmental variations.

1) Longitudinal Speed

Firstly, vehicle motion is characterised by considering its longitudinal dynamics. Time intervals associated with vehicle stopping at road traffic lights were excluded to ensure that speed variability reflected driver behaviour and not external disturbances. To this end, the vehicle's longitudinal speed was inspected together with video recordings from the eye-tracker, discarding time intervals related to traffic lights with zero longitudinal speed. The mean and standard deviation of longitudinal speed have been computed.

2) Standard Deviation of Lateral Position (SDLP)

The vehicle's lateral dynamics was reconstructed by combining the vehicle's Center of Gravity (CG) coordinates and a reference centerline path. The centerline was pre-recorded using a virtual camera mounted on the simulated vehicle's front bumper, moving at 10 km/h to minimise inertial effects. The camera registered the lane left and right lines' positions in a local reference system centred on the vehicle CG. Given discontinuities in the left lane boundary, the right lane was used as a reference, and the centerline was calculated assuming a fixed lane width. The lane left and right lines obtained in the local reference system were transformed into a global reference system common to all participants, for comparison purposes. The SDLP [31] was then computed employing the following equation.

$$SDLP = \mathrm{std}\left(|y_{\mathrm{CM}} - y_{\mathrm{road}}| \cdot \cos(\psi)\right) \tag{1}$$

y_{CM} is the lateral position of the vehicle CM, y_{road} is the centerline position, and ψ is the vehicle yaw angle.

3) Steering wheel grip force

The Instrumented Steering Wheel (ISW) enables the measurement of forces and torques applied by each hand at its respective handle, including the exerted grip force [32]. Processing phases comprised the following steps:

a) Signal zeroing and offset removal.

b) Compensation of the weight force and the inertia force components of the ISW handles [29].

c) Application of a digital zero-phase low-pass filter with a cutoff frequency of 2Hz, to reduce high-frequency noise unrelated to steering actions.

The mean grip force and its standard deviation were then calculated separately for the left and right hands. For the ISW analysis, shorter 8-second segments within the 30-second windows were used to isolate distraction-specific effects. This allowed to minimize the influence of road-induced or transient driving behaviours.

B. Behavioural measurements

Behavioural measurements focused on gaze orientation and oculomotor activity. In particular, the Eyes-Off-Road Time (EORT), the rate of high-velocity eye movements, and the mean duration of low-velocity eye movements were computed for the two considered driving phases (i.e., B and D) through the following steps:

a) *Blink detection and signal correction:* A Hampel filter was applied to the vertical (y-axis) gaze coordinates to detect outliers typically caused by eyelid closures. For each detected blink, a 400ms segment centered on the blink and corresponding to its typical duration [33], was removed from the gaze data and then restored by linear interpolation.

b) *Scene segmentation and EORT estimation:* Each video frame recorded using the eye tracker system was partitioned using a coarser spatial grid. The brightness and RGB colour distributions were then computed within each cell, allowing for the segmentation of on-road versus off-road areas. EORT was then calculated as the proportion of gaze points falling in the off-road region of interest.

c) *Velocity-based gaze movement classification:* Gaze movements were classified using the I-VT (Velocity Threshold) filter based on their angular velocity [34]. In particular, movements with velocities below 30°/s were labelled as low-velocity eye movements, comprising both fixations and smooth pursuits. Those exceeding 100°/s were classified as high-velocity eye movements, attributable to saccades [35].

These measurements rely on gaze parameters that are not restricted to professional-grade wearable eye-tracking setups. The sampling rate adopted in this study (i.e., 25 Hz) matches

This article has been accepted for publication in IEEE Open Journal of Intelligent Transportation Systems. This is the author's version which has not been fully edited and content may change prior to final publication. Citation information: DOI 10.1109/OJITS.2026.3713602

the scene-camera frame rate of the Tobii Pro Glasses 3 and is comparable to the frame rate of standard automotive in-cabin cameras used in vision-based driver monitoring systems [20]. Camera-based gaze estimation algorithms operating without dedicated eye-tracking glasses have been proposed in the literature [20]. Low-cost systems based on eye-tracking devices mounted inside the car cockpit showed the ability to measure both high-velocity and low-velocity eye movements, as well as gaze coordinates [36]. For future VICODEV deployment in naturalistic driving contexts, eye-tracking data quality must be monitored. Beyond sampling frequency, relevant parameters to consider when assessing eye-tracker data quality are scene illumination and subject-dependent calibration [37].

C. Physiological measurements

Physiological signals included Electrocardiogram (ECG) and Electroencephalogram (EEG) recordings, both acquired at 1000Hz. A comprehensive description of filtering, measurement extraction, and artefact removal methodologies is provided in [46]. Subjects 11 and 24 were excluded from EEG and ECG analyses, respectively, due to insufficient signal quality. In this study, physiological measurements are combined with subjective measurements to provide insights that would not otherwise be available with subjective measurements alone, providing further evidence of the effectiveness of the experimental protocol.

1) Electrocardiogram (ECG)

ECG signals were analysed by detecting the R-peaks (i.e., heartbeats) using the Pan-Tompkins algorithm [47]. The time intervals between successive R-peaks, referred to as RR intervals, were then refined using the artefact correction method validated by Lipponen et al. to account for possible ectopic beats and misdetections, yielding a corrected series of Normal-to-Normal (NN) intervals [48].

Time-domain metrics were computed, including the MeanNN interval and the Root Mean Square of Successive Differences (RMSSD) of NN intervals [49]. Frequency-domain features, including the Low-Frequency (LF) and High-Frequency (HF), band powers of heart rate variability (HRV), were also computed, allowing for the estimation of the sympathetic and parasympathetic activity of the autonomic nervous system. Given the relatively short time windows at disposal, frequency-domain analysis was performed using the Point Process model for HRV analysis described in [50], [51]. In particular, the median estimated value of HF and LF power was computed in each analysis window.

2) Electroencephalogram (EEG)

EEG signals were bandpass filtered between 1–30 Hz, and re-referenced to the Common Average. Artefacts were removed using a combination of Artefact Subspace Reconstruction (ASR) [52] and Independent Component Analysis (ICA) [53]. Following ICA, artifactual ocular components were removed using the ICLabel neural network [54]. Conversely, artifactual cardiac components were identified by computing their cross-correlation with ECG data.

Spectral features were then estimated (Welch method, 3s segments, 50% overlap), including power in the theta, alpha, and beta bands [15], as well as relevant band power ratios, as detailed in Table 1. The analysis focused on frontal and parietal regions of interest (ROIs), which were selected based on previous studies highlighting their involvement in attentional processes and cognitive workload [55]–[57].

D. Subjective measurements

Subjective measurements were collected through validated questionnaires, administered to participants before and after the driving simulation. These measurements provided complementary insights into drivers' cognitive state and perceived workload. An in-depth driver psychological state analysis exceeds the scope of this research.

1) Attention Network Test (ANT)

The ANT was employed to describe the tested population's attentional characteristics, evaluating the efficiency of three drivers' attentional networks, namely alerting, orienting, and executive control (i.e., conflict) [26]. The procedure involved a computer-based reaction time (RT) task before the driving simulation, during which drivers received visual stimuli. Alerting refers to the driver's ability to respond to visual stimuli with light aids. Orienting describes the driver's ability to respond to visual stimuli with aids that contain information about the position of the stimulus. Finally, conflict represents the driver's ability to respond to visual stimuli with distractors. ANT were used to characterise drivers' baseline attentional profile, related to induced distraction responses.

2) NASA Task Load Index (NASA-TLX)

The NASA-TLX questionnaire was used to measure subjective workload throughout the simulation [27], [58]. The questionnaire was administered only after the simulation and not between the two driving phases (i.e., B, D) in order to preserve the realism of the simulation and, therefore, the ecological validity of the study. Filling the questionnaire, participants rated six subscales, namely mental demand, physical demand, temporal demand, performance, effort and frustration.

IV. Data analysis

The dataset supporting the findings of this study (i.e., vehicular, behavioural, physiological and subjective measurement results) is available at [59].

A. Statistical analysis

This section describes the statistical methodology adopted to evaluate the significance of trends observed in the ex-

IEEE Open Journal of Intelligent Transportation Systems

Measurement type	Sensor or device	Measurement	Units	Description	Trend	Ref
Vehicular	Vehicle CAN	Mean Longitudinal Speed	m/s	Average longitudinal speed during driving.	↓	[30]
		Standard Deviation of Longitudinal Speed	m/s	Variability of the longitudinal speed during driving.	-	-
		Standard Deviation of Lateral Position (SDLP)	m	Variability of lateral deviation from lane centerline.	↑	[13]
	Instrumented Steering Wheel (ISW)	Mean Grip Force	N	Average grip force applied by the left and right hands on the steering wheel.	↑	[38]
		Standard Deviation Grip Force	N	Variability of grip force applied by the left and right hands.	-	-
Behavioural	Eye Tracker Tobii Pro Glasses 3	Eyes Off Road Time (EORT)	%	Percentage of time with gaze directed away from the road.	↑	[39]
		Mean duration of low-velocity eye movements	s	Average duration of low-velocity eye movements (i.e., fixations and smooth pursuits) within the considered analysis window.	-	-
		Rate of high-velocity eye movements	Hz	Rate of high-velocity eye movements (i.e. saccades) within the considered analysis window.	↑	[40]
Physiological	Electrocardiograph VI-Grade ECG vest	MeanNN Interval	ms	Average interval between successive normal R-peaks (i.e., heartbeats).	↓	[41], [42]
		RMSSD	ms	Heart rate variability measured by Root Mean Square of Successive Differences of NN intervals.	↓	
		LF power	ms^2	Estimated low-frequency (0.04-0.15Hz) HRV power, reflecting the sympathetic branch.	-	-
		HF power	ms^2	Estimated high-frequency (0.15-0.4Hz) HRV power, reflecting parasympathetic branch.	-	-
		LF/HF	-	Ratio between HF power and LF power, index of sympathovagal balance.	-	-
	Electroencephalograph ANT Neuro NA-261-waveguard™ net	Relative α_F Power	-	Relative EEG power in the alpha band (8–12Hz) in the frontal region of interest (ROI).	-	-
		Relative β_F Power	-	Relative EEG power in the beta band (13–30Hz) in the frontal ROI.	↑	[9], [43]–[45]
		Relative θ_F Power	-	Relative EEG power in the theta band (4–8Hz) in the frontal ROI.	↑	
		Relative α_P Power	-	Relative EEG power in the alpha band (8–12Hz) in the parietal ROI.	↓	
		Relative β_P Power	-	Relative EEG power in the beta band (13–30Hz) in the parietal ROI.	↑	
		Relative θ_P Power	-	Relative EEG power in the theta band (4–8 Hz) in the parietal ROI.	↑	
		θ_F/β_F Ratio	-	Ratio of theta to beta power in the frontal ROI.	↓	
		θ_F/α_P Ratio	-	Ratio of theta frontal to alpha parietal power, referred to as Task Load Index (TLI).	↑	

TABLE 1: List of all measurements retrieved during the experimental campaign. The symbols ”↑” and ”↓” indicate a measurement respectively expected to increase or decrease during visual-cognitive distraction. The symbol ”-” shows no shared trend in the literature.

Measurement type	Measurement	*N*	Tail	Raw p-value	Adjusted p-value	Effect size	Variation
Vehicular	Mean Longitudinal Speed	35	Left	1.41×10^{-7}	1.46×10^{-6}	-0.84	-19%
	Standard Deviation of Longitudinal Speed	35	Both	2.44×10^{-4}	6.39×10^{-4}	0.66	14%
	Standard Deviation of Lateral Position	35	Right	1.29×10^{-7}	1.46×10^{-6}	0.87	100%
	Standard Deviation Grip Force	35	Both	5.63×10^{-3}	1.07×10^{-2}	0.47	33%
Behavioural	Eyes Off-Road Time	35	Right	2.53×10^{-6}	1.07×10^{-5}	0.77	100%
	Rate of high-velocity eye movements	35	Right	2.90×10^{-5}	8.69×10^{-5}	0.68	27%
	Mean duration of low-velocity eye movements	35	Both	2.03×10^{-6}	1.06×10^{-5}	-0.80	-39%
Physiological	MeanNN Interval	34	Left	2.09×10^{-7}	1.46×10^{-6}	-0.87	-7%
	RMSSD	34	Left	2.73×10^{-5}	8.69×10^{-5}	-0.69	-23%
	Relative α_F Power	18	Both	3.38×10^{-2}	6.20×10^{-2}	-0.49	-1%
	Relative α_P Power	18	Both	6.50×10^{-3}	8.08×10^{-3}	-0.64	-1%
	Relative β_P Power	18	Right	1.18×10^{-2}	2.05×10^{-2}	0.53	7%
	θ_F/α_P Ratio (Task Load Index)	18	Right	4.49×10^{-3}	9.42×10^{-3}	0.62	10%

TABLE 2: Measurements showing statistical significance (i.e., raw p-value < 0.05) among measurements collected during the experimental campaign. For each measurement, the number of subjects included in the analysis (N), the test tail, the raw p-value, the p-value adjusted for multiple comparisons ($m = 21$) via the Benjamini-Hochberg procedure (False Discovery Rate set to 5%), the effect size, and the relative variation with respect to the baseline (i.e., normal driving) are provided.

perimental measurements across the non-induced distraction baseline (B) and induced Distraction (D) driving phases.

1) Methodology

Statistical analysis was conducted on the extracted vehicular, behavioural, and physiological measurements. The flowchart of the subject pool for each sensor is detailed in Figure 4. For each subject, the values of each measurement were averaged across repetitions of the same driving phase. The Wilcoxon signed-rank test was then used to assess differences in medians between B and D driving phases (Figure 2). Depending on prior literature, as detailed in Table 1, one-sided (i.e., left or right) or two-sided tests were applied. A significance level $\alpha = 0.05$ was used. The Benjamini-Hochberg (BH) correction has been considered to account for multiple comparisons [60]. Finally, the effect size $r = Z/\sqrt{N}$ was computed to quantify the strength of the observed effects [61].

2) Results

Table 2 lists the measurements showing statistical significance, considering raw p-values. The statistical analysis showed that 12 out of 21 measurements exhibited significant differences after Benjamini-Hochberg (BH) p-value correction (i.e., adjusted p-value < 0.05) between the non-induced distraction baseline (B) and the induced distraction (D) phases. Relative α_F power lost significance following BH correction. These measurements spanned all measurement types and sensors. Results were generally consistent across subjects and aligned with findings in the literature. This experimental campaign confirmed trends in Table 1. Considering both p-values and effect sizes, the most significant results were obtained from vehicular and behavioural measures. Notably, these measurements are also easier to collect in real-world driving conditions, supporting the study's practical relevance. It is relevant to highlight the reduction of the mean duration of low-velocity eye movements. This trend has been observed in the literature during visual-cognitive distractions due to gaze fragmentation as an adaptive attempt to follow primary and secondary tasks rapidly [10]. Finally, EEG measurements were derived from a smaller population sample, which may account for their relatively lower statistical significance.

Subjective Test	Measurement	Mean	Median	SD
Attention Network Test	Alerting	41.73	43.75	27.03
	Orienting	46.24	50.00	26.84
	Conflict	61.72	58.75	26.22
NASA-TLX Questionnaire	Mental	78	80	14
	Physical	26	25	21
	Temporal	60	60	24
	Performance	45	40	29
	Effort	57	60	22
	Frustration	40	55	33

TABLE 3: Subjective measurements results from the Attention Network Test (ANT) and the NASA-TLX questionnaire.

B. Descriptive analysis

Subjective measurement results obtained from the ANT and NASA-TLX questionnaire have been analysed using descrip-

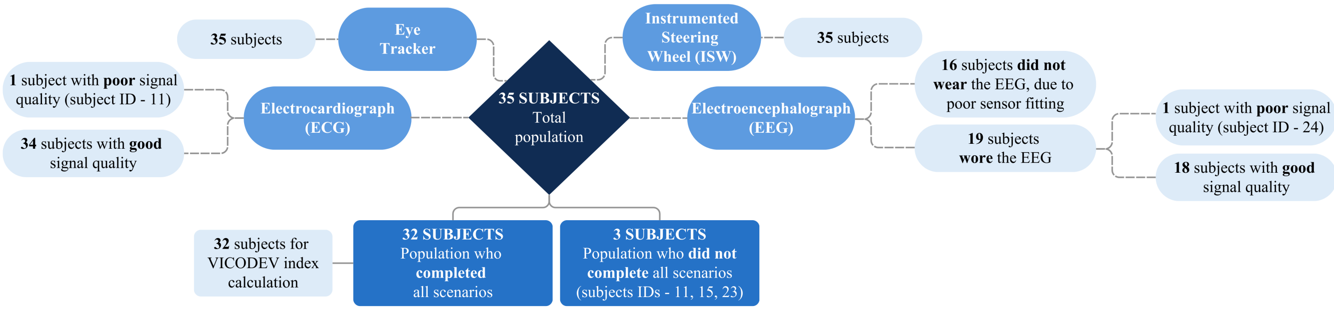

FIGURE 4: Flowchart detailing subjects available for each sensor employed and for VICODEV index calculation.

tive statistics. Table 3 lists the subjective measurements' mean, median and standard deviation.

Results suggest that the study population includes individuals with difficulties in managing conflicts and focusing attention on a determined task (i.e., high conflict). Furthermore, drivers reported high mental and temporal demands. These results may be related to the cognitive workload associated with mathematical computation and the high pressure to respect the allocated time during the clock task. This is supported by EEG results shown in Table 2, highlighting increased workload during induced visual-cognitive distraction.

Finally, the rate of correct and incorrect calculations of each participant was tracked during the test. 80% of the calculations with Arabic numerals were correct, compared to 55% of the calculations with Roman numerals. This confirms the increased complexity in the clock sequence.

V. VICODEV INDEX: A HYBRID METRIC FOR DISTRACTION ASSESSMENT

Before introducing the "VIsual-COgnitive Distraction through Eye-tracking and Vehicular measurements" (VICODEV) index, it is essential to clarify the key hypothesis behind its development. Although the experimental protocol was designed to induce visual-cognitive distraction, it cannot be assumed that all participants experienced it. Some may have ignored the secondary task, prioritised driving, or completed the task without significant cognitive effort. On the other hand, it is reasonable to assume that the population experienced induced visual-cognitive distraction. For this reason, the index aims primarily to detect consistent response patterns across the entire population rather than to assess visual-cognitive distraction at the individual level.

A. Signal selection

VICODEV relies solely on the five vehicular and behavioural measurements detailed in Table 5. This decision was made considering data robustness and measurements' real-time in-vehicle applicability (i.e., the possibility of easily taking measurements on board the vehicle). Only participants who completed distraction-event repetitions and had good-quality data were considered. As shown in Figure 4, 32 subjects were included, excluding subjects 11, 15, and 23.

B. Weights calculation

The VICODEV index linearly combines the selected measurements as follows.

$$VICODEV = \sum_{i=1}^{5} w_i \times M_i \tag{2}$$

where w_i are the weights of the linear combination associated with the M_i selected measurements. The following method was applied to obtain the weights w_i.

1) A multivariate analysis of variance (MANOVA) quantifies how much each measurement changes between the normal and the induced distracted driving while accounting for the correlations among signals [62].
2) A canonical discriminant (i.e., canonical variate) analysis converts the MANOVA results into weights w_i [63].

When performing the validation procedure, the weights w_i were estimated on the training folds and applied unchanged to the test fold, as described in Section V-D.

C. Normalisation and smoothing

Measurements used for the final VICODEV calculation are the average among participants. Their time histories were computed using a sliding window approach and resampled with a time step of 0.04 seconds (i.e., 25 Hz) to match the sampling frequency of the eye-tracker data. Furthermore, to enable a consistent combination of measurements with different units of measure and ranges, the signals were normalised between 0 and 1. Finally, a real-time first-order Infinite Impulse Response (IIR) filter was applied to smooth the raw index values, mitigating potential high-frequency fluctuations while preserving responsiveness.

When performing the validation procedure, the normalisation values were computed on the training folds and applied unchanged to the test fold, as described in Section V-D

D. Validation procedure

The VICODEV index was assessed using two distinct cross-validation strategies, considering (i) the consistency across

This article has been accepted for publication in IEEE Open Journal of Intelligent Transportation Systems. This is the author's version which has not been fully edited and content may change prior to final publication. Citation information: DOI 10.1109/OJITS.2026.3713602

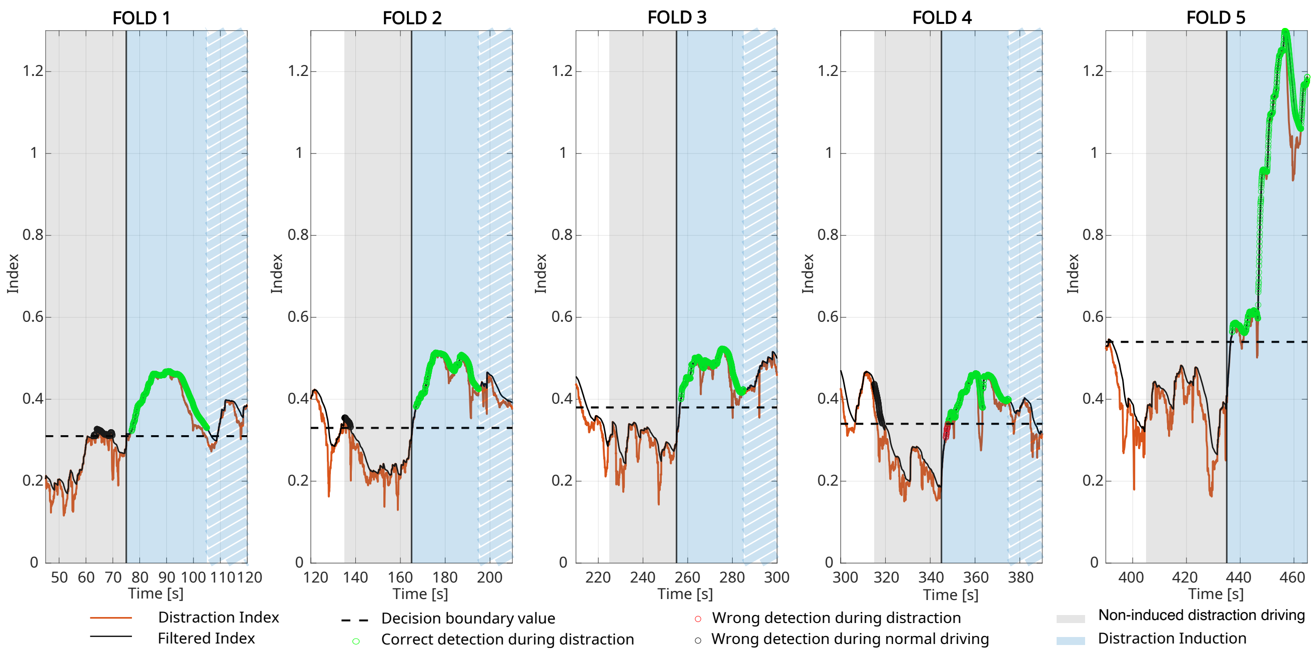

FIGURE 5: Results of the leave-one-repetition-out cross-validation procedure used to check the consistency of the index across the experiment repetitions. In every panel, the filtered distraction index is evaluated on the fold excluded from training. Solid grey and light blue areas indicate phases of normal and induced distraction driving, respectively. White and light-blue striped regions correspond to the time intervals not considered for the evaluation, as detailed in Section III.

the experiment repetitions and (ii) the representativeness of the captured patterns across the tested population. The present validation should be interpreted as specific to the induced Clock-Task-based visual-cognitive distraction.

VICODEV produces a continuous graded output reflecting changes in the driver's distraction state over time, in contrast with most existing methods that formulate distraction detection as a binary task. The current evaluation was nevertheless conducted within a binary classification framework (i.e., normal driving vs induced distraction) as a benchmarking step to enable comparison with the prevailing literature.

For the evaluation, a two-second delay is assumed from the beginning of the clock task to account for drivers' response time [64].

Data partitioning followed the leave-one-repetition-out and leave-one-subject-out cross-validations described in Subsections V-D.1 and V-D.2. To prevent data leakage, all preprocessing and parameter selection steps were performed strictly within the training folds of each iteration. Steps include index weights calculation (Section V-B), normalisation (Section V-C), and decision boundary selection. The resulting weights, normalisation ranges, and decision boundaries were then applied unchanged to the corresponding test fold, used only for evaluation.

Finally, the two cross-validation strategies were considered for the index (i) with all five measurements, (ii) with only SDLP (i.e., a vehicular measurement and the primary outcome of the analysis) and (iii) with only EORT (i.e., a behavioural measurement easily available for vehicular integration).

1) Evaluation of the index consistency across repetitions

A leave-one-repetition-out cross-validation strategy was employed to assess the consistency of the VICODEV index across the five repetitions of the experiment.

In accordance with the hypothesis detailed in Section V, the index was computed using an *average subject* profile derived from the entire experimental population. Specifically, data partitioning was performed iteratively, with the linear model used to compute the index trained on four repetitions of the experiment and tested on the remaining one [66]. Moreover, a decision boundary threshold was optimised on the training repetitions to maximise binary classification accuracy (i.e., normal driving vs. induced visual-cognitive distraction). This evaluation allowed the assessment of both the stability of the discriminant direction (i.e., the index weights) and the consistency of the index scale over time within the considered average subject signal. Table 4 reports the weights obtained in each iteration, along with precision, recall, and accuracy values. Figure 5 shows the index obtained for each tested iteration.

Considering the SDLP alone, a mean accuracy of 61.0%, a mean recall of 50.7%, and a mean precision of 60.9% is obtained. Considering only the EORT, a mean accuracy of

This article has been accepted for publication in IEEE Open Journal of Intelligent Transportation Systems. This is the author's version which has not been fully edited and content may change prior to final publication. Citation information: DOI 10.1109/OJITS.2026.3713602

Measurement	Fold 1	Fold 2	Fold 3	Fold 4	Fold 5
SDLP (w_i)	0.662	0.632	0.537	0.609	0.272
SD Grip Force (w_i)	0.050	0.027	0.004	0.021	0.076
EORT (w_i)	0.044	0.039	0.038	0.023	0.233
Rate of high-velocity eye movements (w_i)	0.034	0.036	0.102	0.067	0.041
Mean duration of low-vel. eye mov. (w_i)	-0.210	-0.267	-0.319	-0.282	-0.378
Decision Boundary Thr.	0.31	0.33	0.38	0.34	0.54
Test Precision	81.7%	90.92%	100.0%	88.51%	100.0%
Test Recall	100.0%	100.0%	100.0%	97.0%	100.0%
Test Accuracy	89.0%	95.0%	100.0%	92.0%	100.0%

TABLE 4: Results of the leave-one-repetition-out evaluation assessing index consistency. The measurement weights (w_i), decision boundary thresholds and test metrics obtained are reported. Test metrics definitions are provided in [65].

86.5%, a mean recall of 84.6%, and a mean precision of 92.1% is obtained. Both single-measurement configurations showed lower consistency across experiment repetitions.

2) Evaluation of the shared trends across participants

A Leave-One-Subject-Out (LOSO) cross-validation was performed to determine whether the proposed index captured shared patterns across the tested population. Data partitioning was performed iteratively, relaxing the hypothesis detailed in Section V, with the model trained on the data of all subjects except one, which was reserved for testing. This analysis focused on the Area Under the Receiver Operating Characteristic Curve (AUC) as the primary metric [65]. The AUC is a threshold-independent metric that evaluates the index's capability to discriminate between normal driving and induced distraction across all possible decision boundary thresholds. The objective of this second evaluation was to assess whether, on average, the index provided representative underlying patterns (i.e., higher values during induced distraction relative to normal driving). This characteristic makes the index suitable for future subject-specific models, where thresholds may be personalised to individual baselines (e.g., subject-specific Machine Learning models). This evaluation resulted in a median AUC value of 82.9% (25th percentile: 71.9%; 75th percentile: 88.9%).

Considering only the SDLP, a median AUC value of 60.91% (25th percentile: 55.8%; 75th percentile: 66.0%) is obtained, showing lower consistency across subjects. Considering only the EORT, a median AUC value of 81.3% (25th percentile: 67.3%; 75th percentile: 94.4%) is obtained, yielding a substantially higher inter-subject variability.

E. VICODEV index

The final VICODEV index, shown in Figure 6, was derived using all induced distraction phases, with weights and normalisation reported in Table 5. SDLP and the mean duration of low-velocity eye movements are the most influential contributors to the final index.

Measurement	w_i	Min / Max
SDLP	0.499	0.011 / 0.447 [m]
SD Grip Force	0.032	1.089 / 4.404 [N]
EORT	0.084	0.069 / 0.382 [%]
Rate of high-vel. eye mov.	0.061	1.985 / 5.932 [Hz]
Mean duration of low-vel. eye mov.	-0.323	0.141 / 0.536 [s]

TABLE 5: Weights (w_i) and min/max values for the final VICODEV index calculation. The mean duration of low-velocity eye movements has a negative sign due to its opposite trend during induced visual-cognitive distraction.

The results of the multivariate analysis, as quantified by a Pillai's trace of 0.7 and a p-value of 5.7153×10^{-14}, indicate a statistically significant overall effect of the driving condition (i.e., normal vs. induced distraction) on the selected measurements.

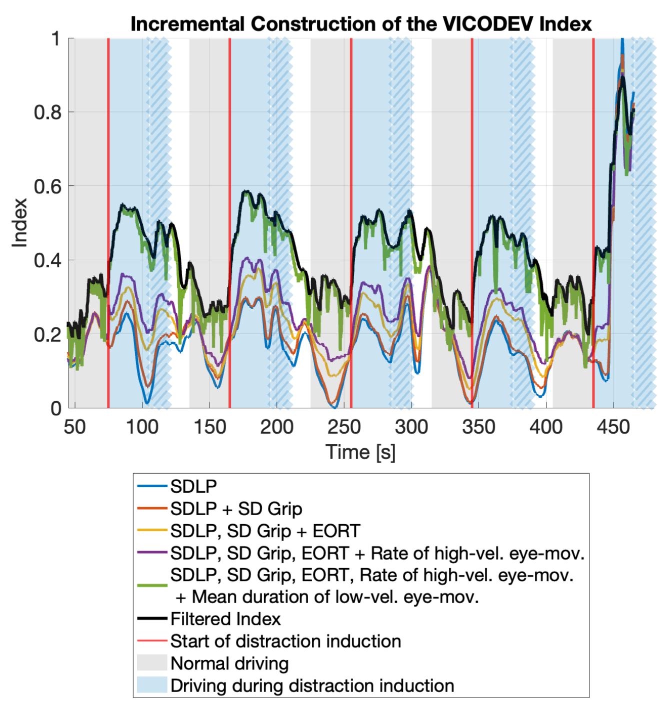

FIGURE 6: Incremental construction of VICODEV index. Each line shows the contribution of each measurement to the index.

VI. Conclusion

Thirty-five participants have been involved in an experimental campaign to detect induced visual-cognitive distraction.

Throughout the driving simulation, participants performed a primary driving task while completing five repetitions of the "Clock Task". During the clock task, drivers summed the values indicated by the clock hands displayed on the vehicle dashboard. This task induced visual-cognitive distraction. Tests were performed in a dynamic driving simulator with an extended sensor setup. Twenty-one vehicular, behavioural, and physiological measurements were extracted. Among these, twelve exhibited statistically significant differences between normal driving and induced distraction phases. This demonstrated the effectiveness and suitability of the selected sensors in capturing induced visual-cognitive distraction. Moreover, subjective assessments demonstrated the presence of cognitive effort during the experiment.

To support real-time application and ensure interpretability, the "VIsual-COgnitive Distraction through Eye-tracking and Vehicular measurements" (VICODEV) index was derived by linearly combining five vehicular and behavioural measurements, i.e., Standard Deviation of Lateral Position (SDLP), grip force standard deviation, Eyes Off-Road Time (EORT), high-velocity eye movement rate, and mean duration of low-velocity eye movements. These measurements have been selected for their robustness and real-time in-vehicle applicability (i.e., the ability to easily measure them on board the vehicle). Physiological measurements were not included in the VICODEV calculation due to current limitations in real-world vehicular integration. Nevertheless, they provided valuable complementary evidence to subjective measurements. Notably, cardiac measurements such as MeanNN and RMSSD of heart rate variability (HRV) showed strong and significant trends. These measurements represent a promising direction to complement VICODEV, given their potential to be acquired via wearable devices. Similarly, EEG measurements, while not directly applicable in real-world driving scenarios, further validated the experimental protocol. Specifically, reductions in EEG relative α_P power and increases in relative β_P power and in the θ_F/α_P Ratio (i.e., Task Load Index) were observed. These variations reflect the increased attentional demand required by the secondary task.

The VICODEV index implementation followed a multivariate statistical procedure, comprising MANOVA and canonical discriminant analysis. This method provides a single optimal projection axis to distinguish between normal driving and induced distracted driving phases. The index was developed to capture consistent response patterns across a population sample. The leave-one-repetition-out cross-validation procedure on the average population subject showed high temporal consistency across the experiment repetitions, with an average recall of 99.47% and accuracy of 95.20%. Further extending VICODEV validation, the leave-one-subject-out cross-validation procedure confirmed the presence of shared discriminative patterns, with a median AUC = 82.9%, Interquartile Range (IQR) 71.9–88.9%. These results indicate that VICODEV could serve both as an interpretable DMS metric and as an informative feature for future subject-specific Machine Learning (ML) models. Furthermore, both validation procedures were performed considering only the SDLP and only the EORT. In the leave-one-repetition-out cross-validation, VICODEV improves recall (+14.87% over EORT, +48.77% over SDLP) and accuracy (+8.7% over EORT, +34.2% over SDLP). In the leave-one-subject-out cross-validation, VICODEV shows a tighter AUC distribution than EORT and a substantially higher median AUC value than SDLP. Generally, VICODEV provides higher and more uniform performance across subjects, with worst-performing subjects scoring higher. These outcomes are consistent with the VICODEV design hypothesis of capturing shared population patterns.

Future developments will aim to employ lower-cost eye-tracking systems, leveraging the scalability of the adopted measurements to more accessible hardware setups. In addition, future work may aim to incorporate subject-dependent variability through subjective measurements. This evolution will benefit from collaborations with psychologists and psychometrists, enabling VICODEV to reflect individual sensitivity to distraction. The current validation was conducted on a homogeneous population of young novice drivers. This allowed controlling for potential confounding effects associated with driving experience or age-related differences in attentional strategies. In this regard, future implementations will aim to extend the validation to more diverse participant pools (e.g., various drivers' ages or experiences). Moreover, future work will aim to extend VICODEV validation toward fully continuous applications, verifying its capabilities to predict distraction and discern between different levels of driver distraction. Finally, VICODEV is currently validated under the specific visual-cognitive distraction induced by the clock task. Future developments will expand its validation across diverse naturalistic non-driving secondary tasks.

ACKNOWLEDGMENT

CSI SpA is greatly acknowledged for its collaboration. Particular acknowledgement is extended to Ing. Ivan Zaffaroni for his valuable assistance and constructive feedback.

REFERENCES

[1] J. J. Rolison *et al.*, "What are the factors that contribute to road accidents? An assessment of law enforcement views, ordinary drivers' opinions, and road accident records." *Accident Analysis & Prevention*, vol. 115, pp. 11–24, 2018.

[2] H. Wei *et al.*, "Quantification of safety improvements and human-machine tradeoffs in the transition to automated driving." *Accident Analysis & Prevention*, vol. 199, p. 107523, 2024.

[3] L. Jin *et al.*, "Impact of non-driving related task types, request modalities, and automation on driver takeover: A meta-analysis," *Safety Science*, vol. 181, p. 106704, 2025.

[4] J. A. Miller *et al.*, "Modeling driver state and takeover behavior in conditional automation using physiological signals," *IEEE Open Journal of Intelligent Transportation Systems*, vol. 7, pp. 477–491, 2026.

[5] United Nations Economic Commission for Europe (UNECE), "Proposal for Supplement 1 to UN Regulation No. 171 on DCAS," https://unece.org/sites/default/files/2024-09/GRVA-20-54e.pdf, Sep. 2024, Paragraph 5.5.4.2. - Accessed: 2025-04-30.

[6] European New Car Assessment Programme (Euro NCAP), "Euro NCAP Vision 2030: A Safer Future for Mobility," https://cdn.euroncap.com/media/74468/euro-ncap-roadmap-vision-2030.pdf, Nov. 2022, Accessed: 2025-04-30.

[7] R. J. Krauzlis *et al.*, "What is attention?" *WIREs Cognitive Science*, vol. 14, no. 1, p. e1570, 2023.

[8] E. Mazzae *et al.*, "NHTSA Driver Distraction Research: Past Present and Future," 2000. [Online]. Available: https://www.researchgate.net/publication/255669554

[9] G. Li *et al.*, "Drivers' EEG Responses to Different Distraction Tasks," *Automotive Innovation*, vol. 6, pp. 20–31, 2 2023.

[10] L. Uccello *et al.*, "From attention to distraction: Driver state analysis from an engineering perspective – a review," *IEEE Access*, vol. 13, pp. 203 286–203 305, 2025.

[11] Z. Qi *et al.*, "A Review of Driver Fatigue Detection and Warning Based on Multi-Information Fusion," in *3rd International Forum on Connected Automated Vehicle Highway System through the China Highway & Transportation Society*. SAE International, dec 2020.

[12] Y. Dong *et al.*, "Driver Inattention Monitoring System for Intelligent Vehicles: A Review," *IEEE Transactions on Intelligent Transportation Systems*, vol. 12, no. 2, pp. 596–614, 2010.

[13] N. M. Yusoff *et al.*, "Selection of Measurement Method for Detection of Driver Visual Cognitive Distraction: A Review," *IEEE Access*, vol. 5, pp. 22 844–22 854, 9 2017.

[14] M. F. A. M. S. Anuar *et al.*, "Transformer architectures for distracted driving behavior detection: A comprehensive review of vision-based approaches," *IEEE Open Journal of Intelligent Transportation Systems*, vol. 7, pp. 233–267, 2026.

[15] G. Li *et al.*, "Driver distraction from the EEG perspective: A review," *IEEE Sensors Journal*, vol. 24, no. 3, pp. 2329–2349, 2023.

[16] A. Abarghooei *et al.*, "Driving Behaviour Detection Using Smart Steering Wheel: Supervised and Unsupervised Classification," *2023 IEEE Sensors Applications Symposium (SAS)*, pp. 1–6, 2023.

[17] H. V. Koay *et al.*, "Detecting and recognizing driver distraction through various data modality using machine learning: A review, recent advances, simplified framework and open challenges (2014 - 2021)," *Engineering Applications of Artificial Intelligence*, vol. 115, p. 105309, 2022.

[18] Y. Ma *et al.*, "Driver Digital Twin for Online Recognition of Distracted Driving Behaviors," *IEEE Transactions on Intelligent Vehicles*, vol. 9, no. 2, pp. 3168–3180, 2024.

[19] K. Yang *et al.*, "Classification and evaluation of driving behavior safety levels: A driving simulation study," *IEEE Open Journal of Intelligent Transportation Systems*, vol. 3, pp. 111–125, 2022.

[20] S. Jha *et al.*, "Driver visual attention estimation using head pose and eye appearance information," *IEEE Open Journal of Intelligent Transportation Systems*, vol. 4, pp. 216–231, 2023.

[21] L. Jin *et al.*, "Mtsf: Multi-scale temporal-spatial fusion network for driver attention prediction," *IEEE Transactions on Intelligent Transportation Systems*, vol. 26, no. 2, pp. 1494–1509, 2025.

[22] H. Yang *et al.*, "Quantitative identification of driver distraction: A weakly supervised contrastive learning approach," *IEEE Transactions on Intelligent Transportation Systems*, vol. 25, pp. 2034–2045, 2024.

[23] DrSMi. (2024) Driving Simulator Politecnico di Milano. Accessed on: Nov. 11, 2024. [Online]. Available: https://www.drismi.polimi.it/

[24] G. Li *et al.*, "A Temporal-Spatial Deep Learning Approach for Driver Distraction Detection Based on EEG Signals," *IEEE Transactions on Automation Science and Engineering*, vol. 19, pp. 2665–2677, 2022.

[25] M. S. Gazzaniga *et al.*, "The cognitive neurosciences," *BMJ*, vol. 312, pp. 193–193, 1996. [Online]. Available: https://api.semanticscholar.org/CorpusID:221931938

[26] A. Olejniczak-Serowiec *et al.*, "Brief-ANT as a tool for measuring the influence of roadside advertisements content on the drivers' attentional processes," vol. 231. EDP Sciences, 11 2018.

[27] S. G. Hart *et al.*, "Development of nasa-tlx (task load index): Results of empirical and theoretical research," in *Advances in psychology*. Elsevier, 1988, vol. 52, pp. 139–183.

[28] G. Previati *et al.*, "Influence of the inertia parameters on a dynamic driving simulator performances," in *81st Annual International Conference on Mass Properties*. Society of Allied Weight Engineers, Inc., 2022.

[29] M. Gobbi *et al.*, "An instrumented steering wheel for driver model development," *Mechatronics*, vol. 64, p. 102285, 12 2019.

[30] B. Fu *et al.*, "A Distracted Driving Detection Model Based on Driving Performance," *IEEE Access*, vol. 11, pp. 26 624–26 636, 2023.

[31] A. Ameyoe *et al.*, "Estimation of Driver Distraction Using the Prediction Error of a Cybernetic Driver Model," 04 2015.

[32] G. Previati *et al.*, "Driver–steering wheel interaction during cornering," *SAE International Journal of Vehicle Dynamics, Stability, and NVH*, vol. 8, no. 3, pp. 427–442, jul 2024.

[33] F. VanderWerf *et al.*, "Eyelid movements: behavioral studies of blinking in humans under different stimulus conditions," *Journal of neurophysiology*, vol. 89, no. 5, 2003.

[34] D. Salvucci *et al.*, "Identifying fixations and saccades in eye-tracking protocols," *Proceedings of the Eye Tracking Research and Applications Symposium*, pp. 71–78, 01 2000.

[35] X.-S. Li *et al.*, "Classification of eye movement and its application in driving based on a refined pre-processing and machine learning algorithm," *IEEE Access*, vol. 9, 2021.

[36] S. Guasconi *et al.*, "A low-cost implementation of an eye tracking system for driver's gaze analysis," in *2017 10th International Conference on Human System Interactions (HSI)*. IEEE, 2017, pp. 264–269.

[37] K. Holmqvist *et al.*, "Eye tracker data quality: What it is and how to measure it," in *Proceedings of the symposium on eye tracking research and applications*, 2012, pp. 45–52.

[38] Y. Sahar *et al.*, "Grip force on steering wheel as a measure of stress," *Frontiers in Psychology*, vol. Volume 12 - 2021, 2021.

[39] X. Wang *et al.*, "Characteristics of driver cell phone use and their influence on driving performance: A naturalistic driving study," *Accident Analysis & Prevention*, vol. 148, 12 2020.

[40] S. L. Kim *et al.*, "Evaluation of the Effects of Driver Distraction Part 1: Based on Simulator Experiments," *2018 IEEE International Conference on Systems, Man, and Cybernetics*, pp. 1081–1086, 2018.

[41] A. Sahayadhas *et al.*, "Physiological signal based detection of driver hypovigilance using higher order spectra," *Expert Systems with Applications*, vol. 42, pp. 8669–8677, 12 2015.

[42] K. A. Brookhuis *et al.*, "Monitoring drivers' mental workload in driving simulators using physiological measures," *Accident Analysis & Prevention*, vol. 42, pp. 898–903, 5 2010.

[43] C. T. Lin *et al.*, "Effects of Multisensory Distractor Interference on Attentional Driving," *IEEE Transactions on Intelligent Transportation Systems*, vol. 23, pp. 10 395–10 403, 8 2022.

[44] C. Shi *et al.*, "Right superior frontal involved in distracted driving," *Transportation Research Part F: Traffic Psychology and Behaviour*, vol. 93, pp. 191–203, 2 2023.

[45] Y.-C. Liu *et al.*, "Human-Machine Interface Evaluation Using EEG in Driving Simulator," in *2023 IEEE Intelligent Vehicles Symposium (IV)*, 2023, pp. 1–6.

[46] M. Gobbi *et al.*, "Objective and subjective evaluation of the interaction of automated vehicles and human drivers in take-over scenarios," SAE Technical Paper, Tech. Rep., 2025.

[47] J. Pan and W. J. Tompkins, "A real-time QRS detection algorithm," *IEEE transactions on Biomedical Engineering*, no. 3, 1985.

[48] J. A. Lipponen *et al.*, "A robust algorithm for heart rate variability time series artefact correction using novel beat classification," *Journal of Medical Engineering & Technology*, vol. 43, pp. 173–181, 2019.

[49] F. Shaffer *et al.*, "An overview of heart rate variability metrics and norms," *Frontiers in public health*, vol. 5, 2017.

[50] R. Barbieri *et al.*, "A point-process model of human heartbeat intervals: new definitions of heart rate and heart rate variability," *American Journal of Physiology-Heart and Circulatory Physiology*, vol. 288, no. 1, 2005.

[51] E. M. Polo *et al.*, "Comparative assessment of physiological responses to emotional elicitation by auditory and visual stimuli," *IEEE Journal of Translational Engineering in Health and Medicine*, 2023.

[52] C.-Y. Chang *et al.*, "Evaluation of artifact subspace reconstruction for automatic artifact components removal in multi-channel EEG recordings," *IEEE Transactions on Biomedical Engineering*, vol. 67, no. 4, 2019.

[53] T. W. Lee *et al.*, "Independent component analysis using an extended infomax algorithm for mixed subgaussian and super-gaussian sources," *Neural computation*, vol. 11, 1999.

[54] L. Pion-Tonachini *et al.*, "ICLabel: An automated electroencephalographic independent component classifier, dataset, and website," *NeuroImage*, vol. 198, 2019.

[55] Y. Wang *et al.*, "Theta and alpha oscillations in attentional interaction during distracted driving," *Frontiers in behavioral neuroscience*, 2018.

[56] S. Coelli *et al.*, "EEG indices correlate with sustained attention performance in patients affected by diffuse axonal injury," *Medical & biological engineering & computing*, vol. 56, 2018.

[57] M. Deng *et al.*, "An analysis of physiological responses as indicators of driver takeover readiness in conditionally automated driving," *Accident Analysis & Prevention*, vol. 195, 2024.

[58] L. Tijerina *et al.*, "An examination of driver eye glance behavior, navigational errors, and subjective assessments while using in-vehicle navigational systems with and without landmark enhancements," vol. 2017-March. SAE International, 3 2017.

[59] L. Uccello *et al.*, "Visual-cognitive distraction in a driving simulator. vehicular, behavioural, physiological and subjective measurements," 2026. [Online]. Available: https://dx.doi.org/10.21227/r8fc-2y40

[60] D. Thissen *et al.*, "Quick and easy implementation of the benjamini-hochberg procedure for controlling the false positive rate in multiple comparisons," *Journal of Educational and Behavioral Statistics*, vol. 27, no. 1, pp. 77–83, 2002.

[61] C. O. Fritz *et al.*, "Effect size estimates: current use, calculations, and interpretation." *Journal of experimental psychology: General*, vol. 141, no. 1, p. 2, 2012.

[62] L. Onyiah, "Multivariate analysis of variance (manova)," *The SAGE Encyclopedia of Research Design*, 2022.

[63] A. C. Rencher, "Interpretation of canonical discriminant functions, canonical variates, and principal components," *The American Statistician*, vol. 46, pp. 217–225, 1992.

[64] J. Du *et al.*, "How is the visual working memory load of driver influenced by information density of traffic signs?" *Transportation Research Part F: Traffic Psychology and Behaviour*, vol. 86, pp. 65–83, 2022.

[65] M. Hossin and M. N. Sulaiman, "A review on evaluation metrics for data classification evaluations," *International journal of data mining & knowledge management process*, vol. 5, no. 2, p. 1, 2015.

[66] G. Chanel *et al.*, "Emotion assessment: Arousal evaluation using EEG's and peripheral physiological signals," in *International workshop on multimedia content representation, classification and security*. Springer, 2006.

Lorenzo Uccello is a Ph.D. researcher at Politecnico di Milano. He received his M.Sc. in Mechanical Engineering, Ground Vehicles, in 2023. His research focuses on Advanced Driver Assistance Systems (ADAS) and Automated Driving (AD) technologies, ranging from communication protocols and cooperative driving to sensor fusion and simulation. He is exploring the effect of the human factor to analyse human-machine interaction, leveraging state-of-the-art sensors

Luca Subitoni is a professional engineer who received his master's degree in Biomedical Engineering, Technologies for Electronics, from Politecnico di Milano in 2023. He pursued a one-year postgraduate research fellowship at the same institution, focusing on human-machine interaction in the field of automated driving. His work focused on machine learning and signal processing, with applications in intelligent systems.

Massimiliano Gobbi received the master's degree (with Hons.) in mechanical engineering and the Ph.D. degree in applied mechanics in 1994 and 1998, respectively. He is currently a Full Professor with the Department of Mechanical Engineering, Politecnico di Milano, Milan, Italy. In 1998, he was a Visiting Scholar with the Department of Mechanical Engineering, University of California Berkeley, Berkeley, CA, USA. He has authored or co-authored more than 200 technical papers. He is the author of seven international patents and three books. His research interests include road vehicle engineering, optimization of complex systems, and mechatronics.

Maria Gabriella Signorini is a Full Professor in the scientific community of Bioengineers at the Department of Electronic, Information and Bioengineering (DEIB), Politecnico di Milano since 2021. With extensive expertise in biomedical signal processing and AI-driven methodologies, her research enhances clinical diagnostics and healthcare technologies, particularly in fetal monitoring, dialysis, and cardiovascular diseases. She founded the interdepartmental DATACLOUD lab, promoting high-computing infrastructures for AI and machine learning applications. Signorini has contributed to innovative biomedical devices and published over 200 scientific papers. She served on Italy's national Committee of Experts for Research Policy and holds editorial roles in leading bioengineering journals, including IEEE-EMBS Conference, Frontiers in Neuroscience, and Computer Methods and Programs in Biomedicine.

Gianpiero Mastinu is full professor of Road and Off-road Vehicles at Politecnico di Milano. Born in Como on August 4th, 1960. Graduated with honours at the Politecnico di Milano (1984). Doctoral degree in Applied Mechanics (1989). Appointed as Full Professor at TU Delft (2000). Full professor at Politecnico di Milano (2004). Co-founder of the Laboratory for Safety of Transport systems (LaST) of the Politecnico di Milano and coordinator of the Active Safety Division. Founder of the Driving Simulator Laboratory of the Politecnico di Milano. Secretary General of the Cluster Mobility of Lombardy (Government of Lombardy Region). Coordinator of the Scientific Board of the National Mobility Cluster of Italy. Member of the EAG of the FIA. Formerly director of the Master "Vehicle Engineering" organized by University of Modena and Politecnico di Milano, (sponsored by primary automotive companies from Emilia and Lombardy). Author of five books and of about 200 papers on International Journals. The scientific activity has focused on the design, construction, and test of machines, structures, and mechanical systems, with particular reference to ground vehicles. Topics: conceptual, functional and structural design (optimization methods); experimental mechanics; modelling and simulation of machines; road and rail vehicle system engineering. Prof. Mastinu was President of the XIX IAVSD Symposium (Milan, Aug 2005).